FULL LENGTH ARTICLE

Coupled single-cell and bulk RNA-seq analysis reveals the engulfment role of endothelial cells in atherosclerosis

Jianxiong Xu [a,1], Jinxuan Wang [a,c,1], Hongping Zhang [a], Yidan Chen [a], Xiaojuan Zhang [a], Ying Zhang [a,d], Ming Xie [d], Jun Xiao [d], Juhui Qiu [a,**], Guixue Wang [a,b,*]

[a] *Key Laboratory for Biorheological Science and Technology of Ministry of Education, State and Local Joint Engineering Laboratory for Vascular Implants, Bioengineering Modern Life Science Experiment Teaching Center of Bioengineering College, Chongqing University, Chongqing 400030, China*
[b] *Jinfeng Laboratory, Chongqing 401329, China*
[c] *School of Basic Medical Sciences, Chengdu Medical College, Chengdu, Sichuan 610500, China*
[d] *Chongqing Emergency Medical Center (Chongqing University Central Hospital), Chongqing 400014, China*

Abstract The clearance of apoptotic cell debris, containing professional phagocytosis and non-professional phagocytosis, is essential for maintaining the homeostasis of healthy tissues. Here, we discovered that endothelial cells could engulf apoptotic cell debris in atherosclerotic plaque. Single-cell RNA sequencing (RNA-seq) has revealed a unique endothelial cell subpopulation in atherosclerosis, which was strongly associated with vascular injury-related pathways. Moreover, integrated analysis of three vascular injury-related RNA-seq datasets showed that the expression of scavenger receptor class B type 1 (SR-B1) was up-regulated and specifically enriched in the phagocytosis pathway under vascular injury circumstances. Single-cell RNA-seq and bulk RNA-seq indicate that SR-B1 was highly expressed in a unique endothelial cell subpopulation of mouse aorta and strongly associated with the reorganization of cellular adherent junctions and cytoskeleton which were necessary for phagocytosis. Furthermore, SR-B1 was strongly required for endothelial cells to engulf apoptotic cell debris in atherosclerotic plaque of both mouse and human aorta. Overall, this study demonstrated that apoptotic cell debris

---

* Corresponding author. Key Laboratory for Biorheological Science and Technology of Ministry of Education, State and Local Joint Engineering Laboratory for Vascular Implants, Bioengineering Modern Life Science Experiment Teaching Center of Bioengineering College, Chongqing University, Chongqing 400030, China.
** Corresponding author.
 E-mail addresses: jhqiu@cqu.edu.cn (J. Qiu), wanggx@cqu.edu.cn (G. Wang).
 Peer review under responsibility of Chongqing Medical University.
 [1] These authors contributed equally to this work.

could be engulfed by endothelial cells through SR-B1 and associated with the reorganization of cellular adherent junctions and cytoskeleton.

Introduction

Atherosclerosis, as chronic inflammation and lipid depositing inducing cardiovascular disease, is the major origin of stroke and myocardial infarction in the world. Lipids such as low-density lipoprotein will accumulate in the subendothelium of the vascular wall, which is the key initiating event of atherosclerosis.[1] The resident lipoprotein and cholesterol that excessively accumulate in endothelial cells (ECs), smooth muscle cells, and macrophages will lead to a pro-inflammatory microenvironment in atherosclerotic plaque.[2] Moreover, the over-loaded lipid and pro-inflammatory mediators result in the death of vascular cells in plaque and lead to an increase in lesion size and the formation of necrotic core,[3,4] which will result in stroke or other cardiovascular diseases.[5,6]

The function and homeostasis of healthy tissues depend on efficiently clearing and replacing billions of apoptotic cells and debris daily during development and adult life.[7] Among the different types of cell death, apoptotic cell death accounts for the majority of cellular turnover, which is an important event in the development of atherosclerotic plaque. Although apoptotic cells or their debris are mainly cleared by professional phagocytes, such as macrophages and neutrophils,[8,9] non-professional phagocytes also play an important role in debris clearance.[10,11] Recent studies have reported that epithelial cells have phagocytic activity to clear apoptotic cells in the early embryo during the absence of specialized immune cells.[12] In addition, our lab found that ECs could engulf and degrade myelin debris after spinal cord injury to promote inflammation and recruit macrophages.[13] Researchers also have detected a huge number of apoptotic cell debris encountered in advanced atherosclerotic areas, suggesting that the removal process of apoptotic materials is insufficient.[14] Thus, we suspected that ECs could act as phagocytes to engulf apoptotic cell debris in advanced atherosclerosis.

Scavenger receptor class B type 1 (SR-B1), also known as Scarb1, is a membrane receptor that participates in cholesterol efflux and carotenoid transportation.[15,16] Furthermore, loss of SR-B1 expression will result in a significant increase in atherosclerotic plaque and lipid-rich necrotic cores in coronary artery.[17] In recent research, SR-B1 has been considered as the binding receptor of low-density protein and is associated with the transcytosis process during atherosclerosis. Meanwhile, specific deletion of SR-B1 in ECs shows a dramatic decrease in atherosclerotic regions.[18] However, loss of SR-B1 expression significantly reduces efferocytosis in macrophages and results in excessive accumulation of dead cells in atherosclerotic lesions.[19] Therefore, we considered that SR-B1 might play an important role in endothelial phagocytosis which was associated with cell debris clearance.

Here, we presented a previously unidentified phenomenon that ECs could engulf apoptotic cell debris in both human and mouse atherosclerotic plaque. Moreover, single-cell RNA sequencing (scRNA-seq) of all cells in the atherosclerotic aorta was further utilized to detect EC heterogeneity and distinct cellular subpopulations with wounding response-relevant functions. Importantly, integrated analysis of three vascular injury-related RNA-seq datasets showed that SR-B1 might play an important role in EC phagocytosis. We also examined that SR-B1 expression was associated with the reorganization of cellular adherent junctions and cytoskeleton. Finally, we demonstrated that SR-B1 as a membrane receptor was essential for recognizing and clearance of apoptotic cell debris in atherosclerotic plaque of both mouse and human aorta (Fig. S1).

Materials and methods

Reagents and antibodies

BLT-1 (HY-116767) was obtained from MCE. DiD (C1039), DAPI (C1002), One Step TUNEL Apoptosis Assay Kit (C1089), and phalloidin-Rhodamine (C2207S) were obtained from Beyotime. Antibodies against Pecam1 (sc-376764) were obtained from Santa Cruz. Antibodies against SR-B1 (ab217318), Goat Anti-Mouse IgG H&L (Alexa Fluor® 488, ab150113), Goat Anti-Rabbit IgG H&L (Alexa Fluor® 555, ab150078), Goat Anti-Rabbit IgG H&L (Alexa Fluor® 647, ab150083), Goat Anti-Mouse IgG H&L (Alexa Fluor® 555, ab150118), and Goat Anti-Mouse IgG H&L (Alexa Fluor® 647, ab150115) were obtained from Abcam.

Animal experiment

All animal experiments were performed according to the guidelines for animal care established by the Chinese Council and approved by the Animal Care and Ethics Committee of Chongqing University. $Apoe^{-/-}$ mice were obtained from Beijing Vital River Laboratory Animal Technology Co., Ltd. Eight-week-old $Apoe^{-/-}$ mice (25−30 g) were fed with a western diet (MD12015 was purchased from Jiangsu Medicine Biomedical Co., Ltd) for 16 weeks to establish advanced atherosclerosis model. All mice were sacrificed at week 24 of the experiment.

Human samples

The collection of human tissues was approved by the institutional review board of Chongqing Emergency Medical Center (Chongqing University Central Hospital, Approval No: Scientific Research 2021(13)), Chongqing, China.

Informed consent was written by patients before enrollment.

Cell culture

Fibronectins (40 μg/mL, Science cell) were coated on cell culture flask 6 h before subculture. Primary human umbilical vein endothelial cells (pHUVECs) were purchased from ScienCell and cultured in endothelial cell medium with 10% fetal bovine serum and endothelial growth supplement (ScienCell) in an incubator set at 37 °C with 5% CO_2.

Preparation of cell debris and *in vitro* uptake assay

To make cell debris, thymocytes were obtained from 8-week-old (25−30 g) C57BL/6 mice. Thymocytes were washed with 0.15 M NaCl and incubated with DiD. Thymocytes were then frozen and thawed three times and centrifuged at 9500 g at 4 °C for 10 min to acquire DiD-labeled cell debris. pHUVECs were seeded in 24-well plates at a density of 1×10^4 cells per well. Cell debris were added to pHUVECs with BLT-1 (1 μM) and 100 μg/mL of cell debris for 3 h. The engulfment number of pHUVECs was calculated by cell debris number/the number of total pHUVECs.

Flow cytometry

pHUVECs were seeded in fibronectin-coated 6-well plates at a density of 1×10^5. Cells were treated with BLT-1 (1 μM) and cell debris for 1 h, 3 h, and 6 h. Then cells were digested by trypsin (Gibco) and centrifuged at 1200 rpm for 10 min to collect cells. The cells were washed with 0.15 M NaCl three times and the mass cells were filtered out by a 40-μm filter membrane. Flow cytometry data were quantified using median fluorescence intensity and plotted by FlowJo software.

Immunofluorescence

Frozen sections of the aortic root and carotid arteries were fixed with 4% paraformaldehyde for 30 min. Cells were fixed with 4% paraformaldehyde for 15 min. The samples were then washed with phosphate buffer saline solution three times and permeabilized with 0.1% Triton X-100 (in phosphate buffer saline solution) for 30 min. The samples were then blocked by 5% bovine serum albumin. Subsequently, the samples were incubated with primary antibody at 4 °C for 12 h, washed with phosphate buffer saline solution three times, and incubated with secondary antibody for 1.5 h. Apoptotic cells were labeled by a TUNEL staining kit obtained from Beyotime. Finally, the cell nuclear was labeled by DAPI. Leica SP8 confocal microscopy was utilized to image the sample.

Analysis of scRNA-Seq data

scRNA-seq data were screened using GEO (http://www.ncbi.nlm.nih.gov/geo) datasets. scRNA-seq datasets GSE155514 and GSE174384 from Pan et al[20] and Kalluri et al[21] were utilized for further analyses. Raw data were processed using R (version 3.8.3) and R package "Seurat V4.0"[22] to trim off cells expressing fewer than 500 genes and genes expressed by less than 3 cells. Cells with expressing genes <500 genes and containing >7.5% mitochondrial genes were considered poor quality and were also discarded. The data then underwent library-size normalization, in which raw gene counts from each cell were normalized relative to the total number of counts. The resulting expression data were then scaled by 10,000 and log-transformed. Subsequently, the normalized data were summarized by principal component analysis and graph-based clustering approach. t-distributed stochastic neighbor embedding (t-SNE) plot was then utilized to visualize the resulting clusters in two dimensions. Finally, cells were classified based on the expression of known biomarkers.

Analysis of RNA-seq data

Vascular injury-related datasets GSE115618,[23] GSE164050,[24] and GSE56143[25] were utilized for further integrated analyses. Bioconductor suite in R packages "limma" and "edgeR" were utilized for the processing of raw data.[26,27] Raw data were firstly calculated as normalized counts for every transcript and counts of genes < 9 in all samples were discarded. The data were then performed linear fit to reduce outliers by package "limma". Differentially expressed genes (DEGs) were performed by pairwise comparison with an FDR < 0.05 in transcript levels.

Analysis of gene ontology (GO) and Kyoto Encyclopedia of Genes and Genomes (KEGG) pathway

DEGs were identified in the RNA-seq datasets by using the "limma" package with logFC > 1 and P-value < 0.05. Subsequently, DEGs were analyzed by R package clusterProfiler to acquire the enriched pathways including GO pathways and KEGG pathways.[28] The biological process of GO pathways and KEGG pathways were enriched with a statistical P-value < 0.05.

Statistical analysis

The data were presented as mean ± standard error of the mean and all experiments were performed with at less of three replications. Two-sided Student's t-test or Tukey's multiple comparison test were utilized to calculate statistical significance between control and experimental groups. The statistically significant difference was indicated as no significance (ns) or significance (*P < 0.05, **P < 0.01, ***P < 0.001, ****P < 0.0001). Three-dimensional images were constructed by Imaris.

Results

ECs contain apoptotic cell debris in both human and mouse atherosclerotic plaque

To prevent inflammatory events in atherosclerotic progression, professional phagocytes are efficiently recruited and participate in efferocytosis and debris clearance.[29] Lipid over-loaded in macrophages may result in foam cell

formation and loss of their phagocytic function.[30] Therefore, non-professional phagocytes are considered to play an important role in clearing cell debris. To determine whether non-professional phagocytes have the ability to clear apoptotic cells in atherosclerotic plaque, immunostaining of western diet (WD)-fed $Apoe^{-/-}$ mice artery revealed that

TUNEL-labeled apoptotic cell debris was localized on intimal Pecam1^{+} ECs (Fig. 1A; Fig. S2A). We also found that human arterial Pecam1^{+} ECs also contained TUNEL-labeled apoptotic cell debris in human atheroma tissues (Fig. 1B; Fig. S2B), suggesting that ECs had the potential to engulf apoptotic cell debris during atherosclerosis. To understand
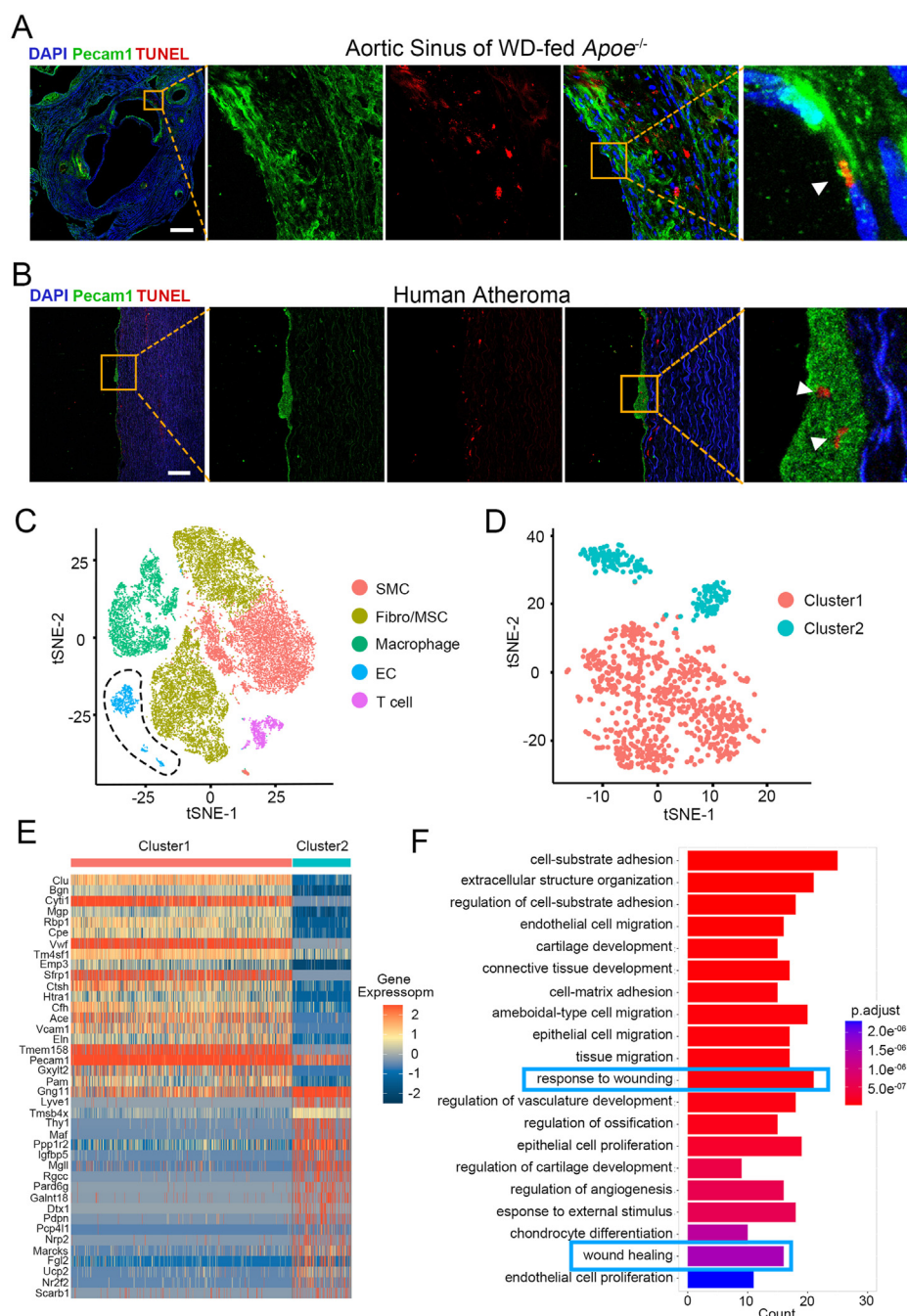

Figure 1 Engulfment of apoptotic cell debris by ECs in atherosclerotic aortas showed unique character via single-cell RNA sequencing. **(A)** Immunostaining for Pecam1 (green) and TUNEL (red) in aortic roots of WD-fed $Apoe^{-/-}$ mice. Scale bar, 400 μm. **(B)** Immunostaining for Pecam1 (green) and TUNEL (red) in human atheroma of patients with atherosclerosis. Scale bar, 200 μm. **(C)** t-SNE plot of single-cell RNA sequencing showed the five identified major aortic cell types from mice fed with WD for 0, 8, 16, and 26 weeks. **(D)** t-SNE plot of two endothelial cell subpopulations distinguished via different transcriptional profiles. **(E)** Gene-expression heatmap of different genes for two endothelial cell subpopulations. Red, high expression; blue, low expression. **(F)** Gene ontology pathway analysis of differentially expressed genes in two endothelial cell subpopulations. WD, western diet; t-SNE, t-distributed stochastic neighbor embedding; EC, endothelial cell; SMC, smooth muscle cell; MSC, mesenchymal stromal cell; Fibro, fibroblast.

the molecular alteration and phenotype transition in ECs, we next analyzed the scRNA-seq dataset GSE155514 provided by Pan et al.,[20] which included ascending aorta, brachiocephalic artery, and thoracic aorta from 0, 8, 16, and 22 weeks WD-fed mice. The artery scRNA-Seq dataset contained 26,028 cells that passed quality filtering (0 week: 6479 cells; 8 weeks: 4056 cells; 16 weeks: 6816 cells; 22 weeks: 8857 cells). Subsequently, the R package (Seurat 4.0) was utilized to construct graph-based clusters and group cells based on the Euclidean distance in PCA space.[23] Then, data was displayed via *t*-SNE plots with ten different clusters (Fig. S3A). Next, we annotated putative biological identities and cell populations based on the expression of different genes, including smooth muscle cells (3 clusters; Acta2, Myh11), mesenchymal stromal cell/fibroblast (3 clusters; Col1a1, Lum), macrophages (2 clusters; Cd68, Cd14), ECs (1 cluster; Pecam1, Vwf), and T cell (1 cluster; Cd27, Rora) (Fig. S3B–K). Thus, individual clusters were labeled with five mainly different cell types with published biomarkers (Fig. 1C).

After the analysis of cell types, we further found that ECs had two distinct groups with obvious *t*-SNE separation (Fig. 1C). Thus, we further investigated the heterogeneity of ECs which could be classified into two clusters and exhibited prominent transcriptomic heterogeneity (Fig. 1D). To further determine whether EC-separated clusters had nonoverlapping transcriptomic profiles, the highest DEGs between cluster 1 and 2 ECs were plotted via heatmap (Fig. 1E). Furthermore, we asked whether EC heterogeneity was due to vascular events and their resulting cellular phenotypical transition. DEGs from cluster 1 and 2 ECs were input into the DAVID bioinformatics database to identify GO terms corresponding to biological processes.[31,32] The results showed that vascular injury-related pathways, such as extracellular structure organization, endothelial cell migration, response to wounding, and wound healing were enriched which indicated that a part of ECs was activated to respond to wounding (Fig. 1F). These results suggested that vascular ECs had the ability to internalize apoptotic cell debris and exhibit an injury-responded phenotype. Thus, we considered that the process of endothelial engulfment was strongly related to vascular injury caused by atherosclerosis.

Identification of DEGs in injured vascular cells reveals multiple signaling pathways, especially cargo receptor activity

The progression of atherosclerosis will result in a number of vascular events including inflammation, endothelial dysfunction, and the formation of necrotic core(s), which may trigger acute vascular injury.[33,34] Using scRNA-seq analysis, we found that vascular injury and repair-related signaling pathways were enriched, which indicated that vascular injury may be an important process of atherosclerosis. Thus, to obtain greater sequencing depth to identify key receptors that regulate cell phagocytosis, we further analyzed the RNA-seq datasets containing mechanical injury, intimal injury, and disturbed flow in the vascular system (GSE115618, GSE164050, GSE56143) from GEO database, which were closely associated with vascular injury. Dataset GSE115618 contained the transcript of endothelial-enriched,

mechanically injured vascular cells after 48 h.[23] Dataset GSE164050 was provided by Bao et al, which included the expression data from vascular cells at two weeks after intimal injury.[24] Moreover, because disturbed blood flow is a key point in the development of atherosclerosis and vascular injury,[35,36] we also analyzed dataset GSE56143, which identified the DEGs from carotid artery ligated mouse ECs (disturbed flow) and control (laminar flow).[25] Then we analyzed the data and drafted the screening standard of our research (adjusted *P* value < 0.05, |Log2 Fold Change| > 1.0). Valco plot showed that 48 h-vascular injury group (GES115618), two weeks-intimal injury group (GSE165050), and vascular ligation group (GSE56143) had a total of 2986, 1216, and 379 up-regulation genes and 1540, 341, and 305 down-regulation genes, respectively (Fig. 2A–C). The heatmap was utilized to display the expression distributions of these DEGs (Fig. 2D–F). Subsequently, to investigate the biological functions of ECs during atherosclerosis and vascular injury, we performed GO enrichment analysis among the three groups (Fig. 2G). The results exhibited that GO pathways, such as extracellular matrix structural constituent and cargo receptor activity, were enriched in all DEG groups and had a high gene ratio and adjusted *p* value. Furthermore, we also analyzed the correlation of the enriched pathway from three DEG groups and found that they had similar enriched pathways and gene expression profiles (Fig. 2H). These results suggested that a part of ECs may played an important role in apoptotic cell clearance during vascular injury in atherosclerosis.

The phagocytosis-like ECs subpopulation in the aorta is coupled to high expression of SR-B1

To better understand how ECs could clear apoptotic cell debris in vascular cells, we further analyzed the KEGG pathways among three vascular injury DEG groups which could indicate the gene expression, gene function, and genome information in the biological process. Integrated analysis of the KEGG pathways showed that phagocytosis-related pathway, FcγR-mediated phagocytosis, and phagosome; proliferation-related pathway, hematopoietic cell lineage, cell cycle, and PI3K-Akt signaling pathway, were enriched (Fig. 3A), which indicated that ECs had a molecular character associated with the phagocytosis and regeneration process. Venn diagram plots were utilized to display a total of 64 consistently expressed genes with adjusted *P* value < 0.05 and |Log2 Fold Change| > 1.0 from the three profile datasets (Fig. 3B and Table S1). These consistently expressed genes were further used to perform on how the phenotypically changed ECs shifted in relation to the vascular injured condition. GO analysis showed that the integrin-mediated signaling pathway, phagocytosis pathway, and cell activation pathway were enriched (Fig. 3C). Because we found that ECs had the ability to engulf apoptotic cell debris in previous work and found that phagocytosis was the main event during vascular injury, we next merged the phagocytosis pathway-related genes to the recently published dataset from Kalluri et al in which scRNA-seq analyze whole aortas from 12-week-old mice.[21] We identified a phagocytosis pathway-related gene Scarb1 (SR-B1) that was specifically highly expressed in ECs
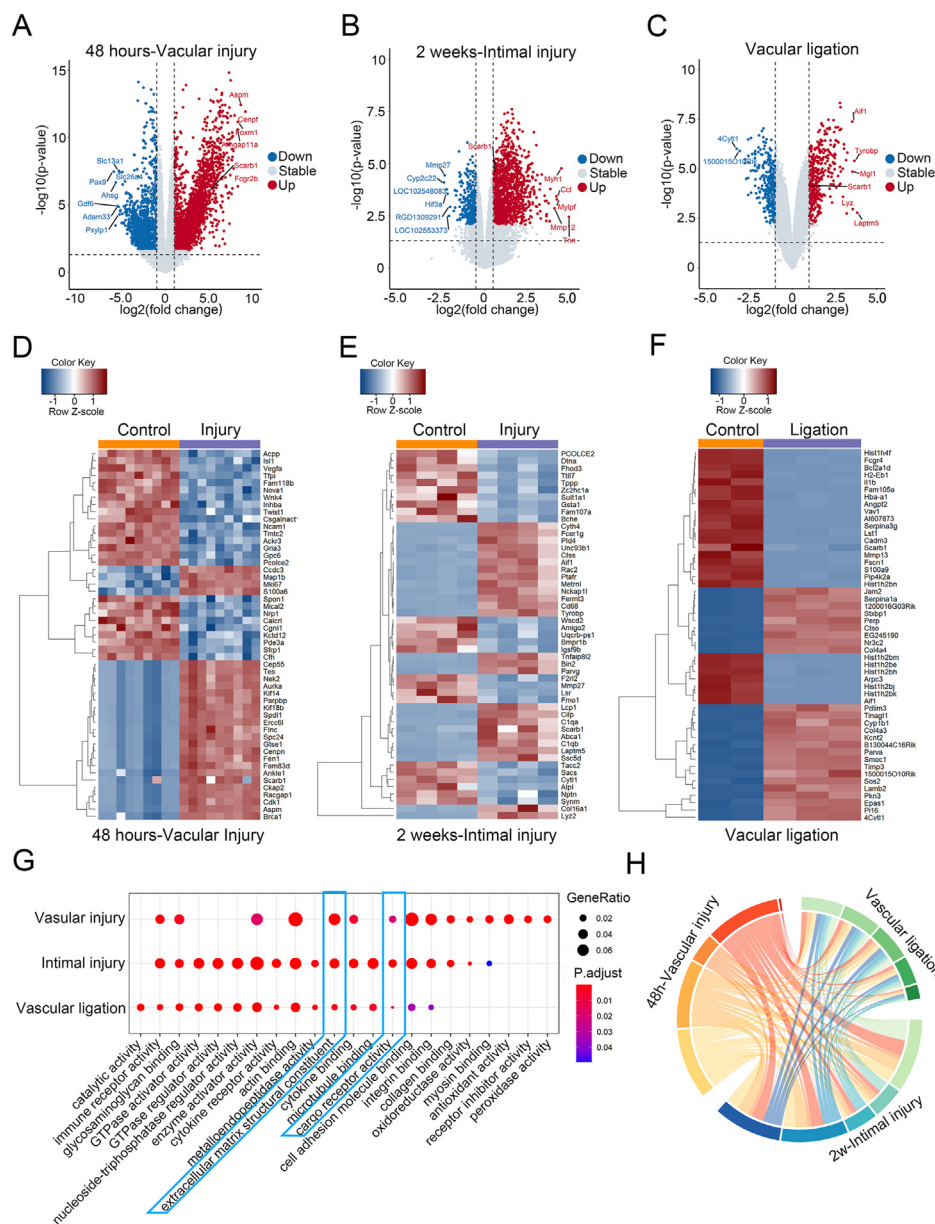
Figure 2 RNA sequencing analysis showed the effect of endothelial cells on responding to vascular injury. **(A)** The volcano plots visualizing the differentially expressed genes (DEGs) of endothelial cells after 48-h vascular injury. **(B)** The volcano plots visualizing the DEGs of vascular cells after two-week vascular intimal injury. **(C)** The volcano plots visualizing the DEGs of endothelial cells after one-week ligation on the carotid artery. **(D)** The heatmap showing the expression level of endothelial cells after 48-h vascular injury. **(E)** The heatmap showing the expression level of vascular cells after two-week vascular intimal injury. **(F)** The heatmap showing the expression level of vascular cells after one-week ligation on the carotid artery. **(G)** Kyoto Encyclopedia of Genes and Genomes pathway enrichment analysis of DEGs in the above three datasets. **(H)** The chord diagram showing the correlation of gene ontology enrichment pathway in the above three datasets.

(Fig. 3D). Thus, we assumed that EC-specifically expressed gene SR-B1 might play an important role in engulfing apoptotic cell debris.

scRNA-seq analysis of vascular ECs identifies SR-B1 high expressed subpopulation in mouse aorta

To linage trace the expressed profile of SR-B1 in vascular ECs, we performed scRNA-seq analysis on the normal fed

and WD-fed mouse aorta. The scRNA-seq dataset containing 5451 cells from normal-fed mouse aorta was acquired from the GEO dataset GSE174384. Furthermore, approximately 4619 cells passed quality control metrics and were utilized to build graph-based clusters and group cells based on the Euclidean distance in PCA space. Unsupervised clustering using R package Seurat4.0 identified 11 cell clusters (Fig. S4A), which annotated cell types based on published markers, including ECs (Pecam1$^+$), smooth muscle cells (Acta2$^+$), mesenchymal stromal cells/fibroblasts (Lum$^+$),
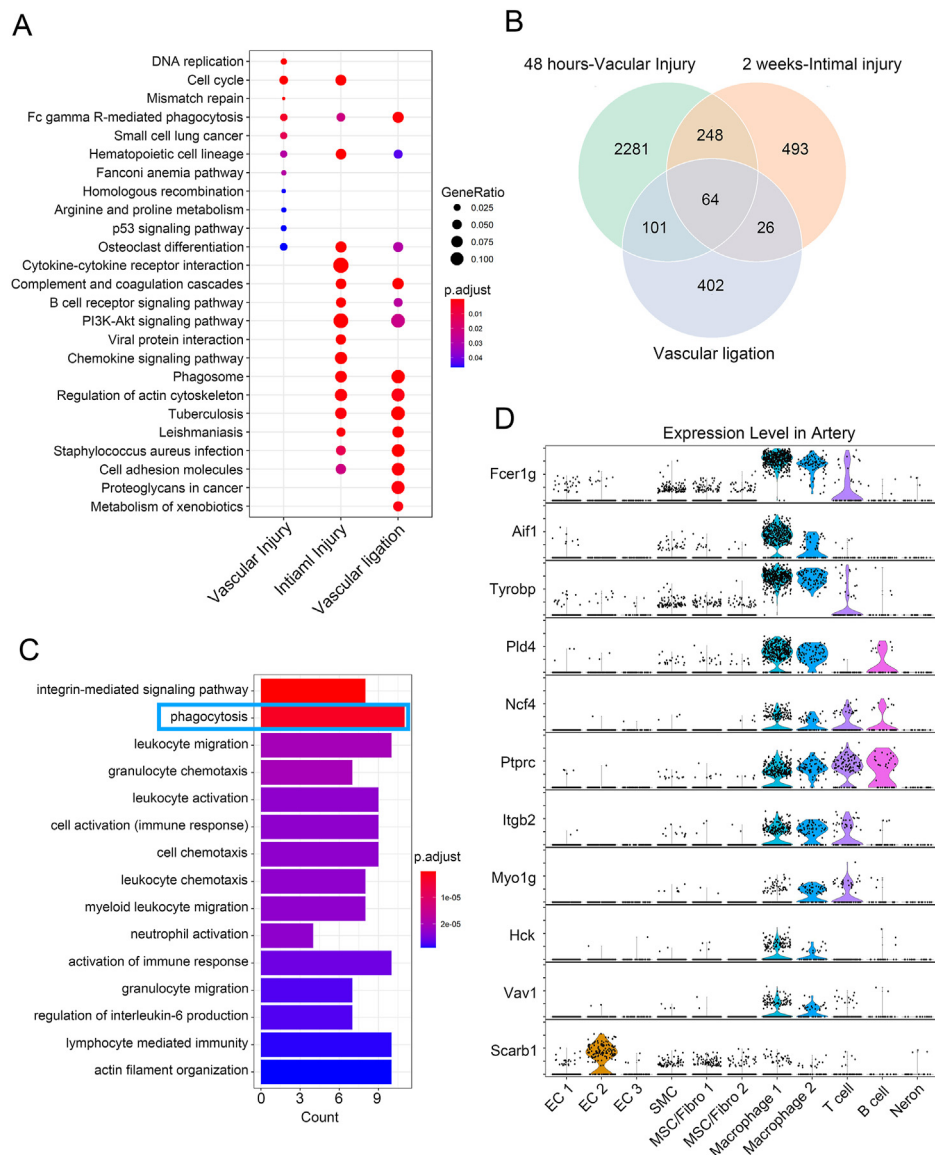
Figure 3 SR-B1 (Scarb1) exhibited increased expression in injured vascular cells and colocalized with aortic endothelial cells. **(A)** Gene ontology pathway enrichment analysis of differentially expressed genes in three vascular injury groups. **(B)** The Venn diagram showing the intersection of differentially expressed genes between three vascular injury groups. **(C)** Top enriched pathways for consistently expressed genes seen with three vascular injury groups. **(D)** The expression of 11 genes associated with enriched pathway-phagocytosis (Fig. 3C) in different arterial cell subpopulations.

macrophages (Cd68$^+$), T cells (Cd3d$^+$), B cells (Cd79a$^+$), and neurons (Gfra3$^+$) (Fig. S4B). After determining the cell type, we identified ten individual groups and found that ECs were clustered into three distinct subpopulations (Fig. 4A). Furthermore, heatmap analysis showed that each of the EC subpopulations had a specific transcriptional profile (Fig. S5). To characterize these three subpopulations, we found that SR-B1 was highly expressed in the EC2 subpopulation (Fig. 4B). Thus, we next addressed the molecular and functional characteristics of these SR-B1 highly expressed cells. Volcano plot showed that 270 genes were significantly up-regulated and 260 genes were down-regulated in SR-B1 highly expressed ECs with naïve ECs (Fig. 4C). To determine the cellular heterogeneity and cellular function of the SR-B1 highly expressed EC subpopulation, GO

enrichment analysis was utilized to identify specifically biological processes (Fig. 4D). We found that the GO terms were associated with the cell junction and cytoskeleton pathway such as positive regulation of cell adhesion, regulation of actin filament-based process, and regulation of actin cytoskeleton organization. Furthermore, the chord diagram exhibited that cellular cytoskeleton- and junction-related genes including Kdr, Tek, Nrp1, Cdh5, Rgcc, and Foxc2 were enriched (Fig. 4E). Moreover, we also found that SR-B1 was highly expressed in a separated EC subpopulation at WD-fed mouse aorta (Fig. S6A). Thus, we analyzed the DEGs in SR-B1 positive and naïve ECs which contained 141 up-regulated genes and 119 down-regulated genes (Fig. S6B). Furthermore, Go analysis also revealed that SR-B1 highly expressed subpopulation have unique
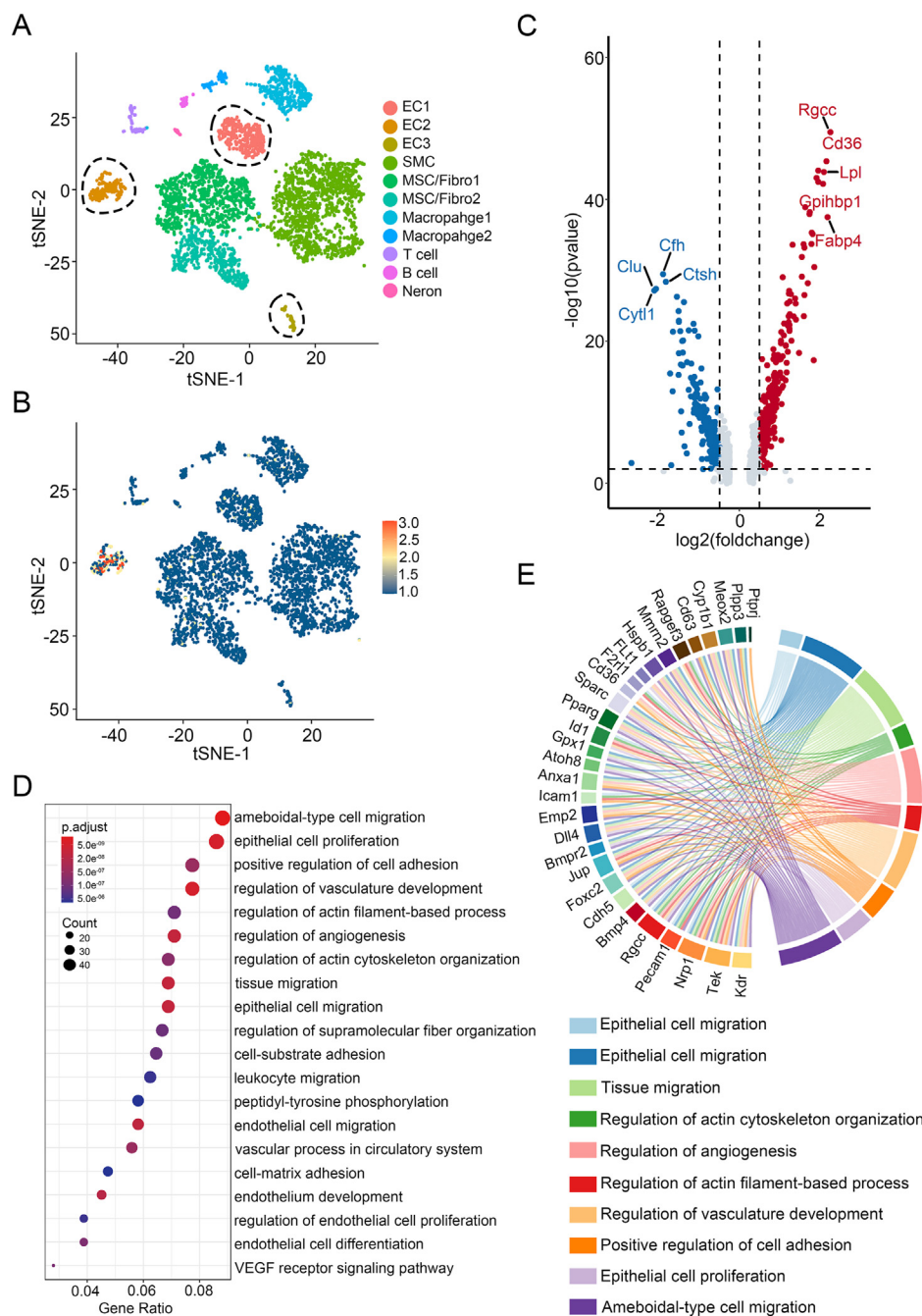
Figure 4 Cellular and molecular characterization of SR-B1-positive endothelial cells in normal-fed mouse aorta. **(A)** *t*-SNE plot of single-cell RNA sequencing from mouse aorta showed seven identified cell types. **(B)** *t*-SNE visualization overlaid with the expression of SR-B1. **(C)** The volcano plots visualizing the differentially expressed genes of SR-B1-positive endothelial cells and naïve endothelial cells. **(D)** Top enriched pathways for gene expression changes seen with SR-B1 highly expressed cells. **(E)** The chord diagram showing the correlation between gene ontology enrichment pathway and differentially expressed genes. *t*-SNE, *t*-distributed stochastic neighbor embedding.

biological processes such as regulation of cell adhesion and regulation of actin cytoskeleton organization, which were similar to the results of scRNA-seq analysis in normal fed mouse aorta (Fig. S7). These results suggested that SR-B1 in the endothelium promoted phagocytosis and debris clearance, which were closely associated with cell junction and cytoskeleton reorganization.

Cellular adherent junctions and cytoskeleton are reorganized in SR-B1 positive ECs during phagocytosis

During GO enrichment analysis, we found that SR-B1-positive ECs had changes in the expression of junction- and cytoskeleton-related genes compared with other ECs.
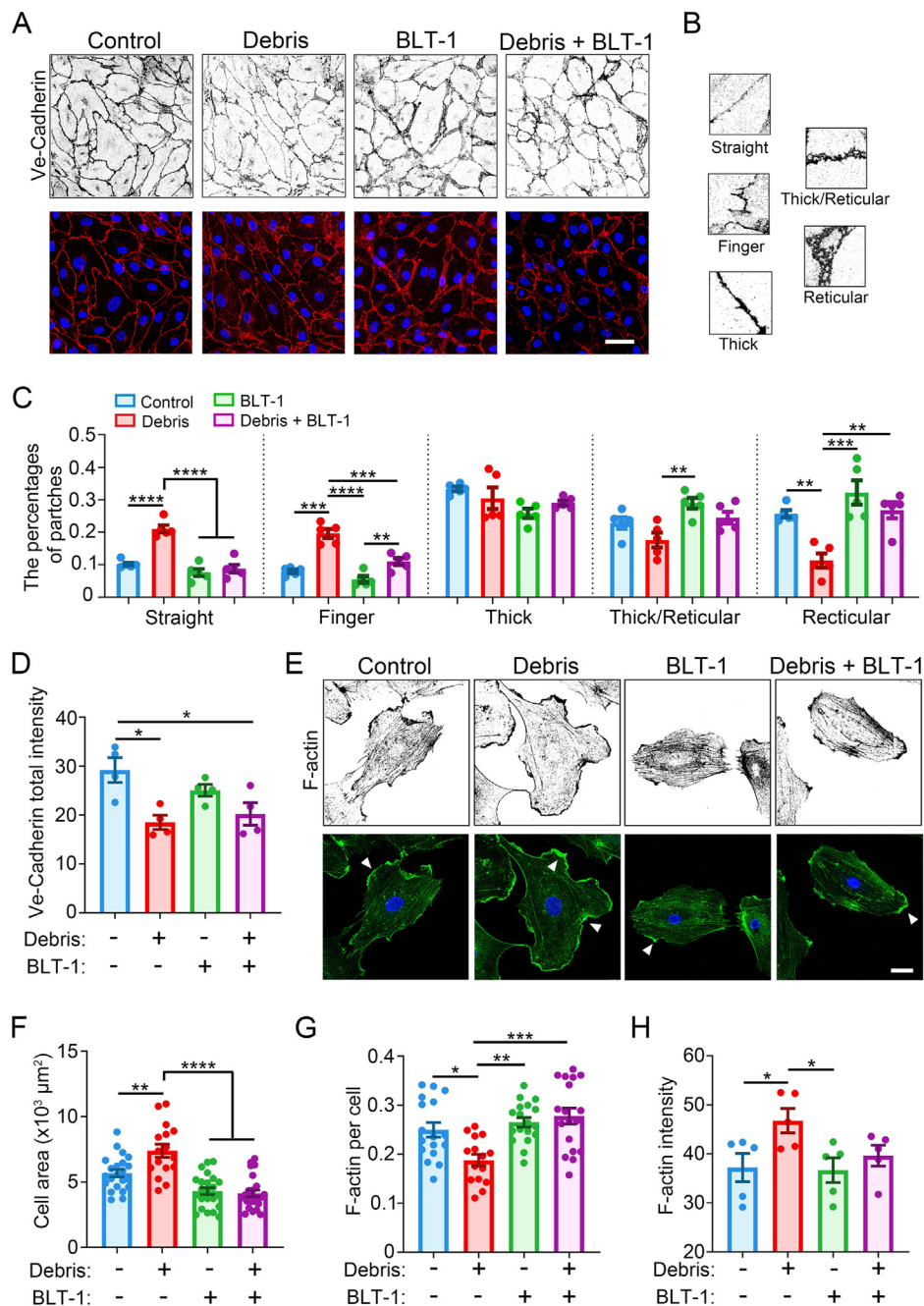
Figure 5 SR-B1 expression and phagocytosis in endothelial cells were associated with the adherent junction and cytoskeleton morphology. **(A)** Immunostaining for VE-Cadherin (red) labeled junctions in primary human umbilical vein endothelial cells (pHUVECs) treated with cell debris and BLT-1. Scale bar, 50 μm. **(B)** Representative images for five morphological classifications of adherent junctions: straight, finger, thick, thick/reticular, and reticular. **(C)** Morphological analysis of VE-Cadherin labeled junctions in pHUVECs treated with cell debris and BLT-1 ($n = 5$). **(D)** Fluorescent intensity of VE-Cadherin in pHUVECs treated with cell debris and BLT-1. **(E)** The representative confocal images showed pHUVECs treated with cell debris and BLT-1 were stained for F-actin by phalloidin (green). White arrowheads, cortical F-actin. Scale bar, 20 μm. **(F)** Quantification analysis of cell area in pHUVECs treated with cell debris and BLT-1 ($n = 15$). **(G)** Quantification analysis of the F-actin distribution in pHUVECs treated with cell debris and BLT-1 ($n = 15$). **(H)** Fluorescent intensity of F-actin in pHUVECs treated with cell debris and BLT-1 ($n = 5$). The data in C, D, F, G, and H were shown as mean ± standard error of the mean (error bars). ns, not significant, $*P < 0.05$, $**P < 0.01$, $***P < 0.001$, $****P < 0.0001$.

Recent studies have revealed that the reorganization of cytoskeleton and adherent junctions cooperated with plasma membrane deformation and remodeling are important for cell phagocytosis.[37–39] Thus we first evaluated the

role of adherent junction and cytoskeleton morphology and stability during EC phagocytosis. VE-Cadherin, as an adherent junction molecule, plays an important role in vascular permeability.[40] Thus, VE-Cadherin staining in

pHUVECs was utilized to further discover the alteration of junctional morphologies. A recent study has reported that there are five VE-cadherin junctional categories: straight, finger, thick, thick/reticular, and reticular (Fig. 6B). The straight and finger types represent that the junctions between ECs are not tight enough and unstable. In contrast, the thick, thick/reticular, and reticular types represent stable VE-Cadherin.[41,42] Imaging analysis of VE-cadherin
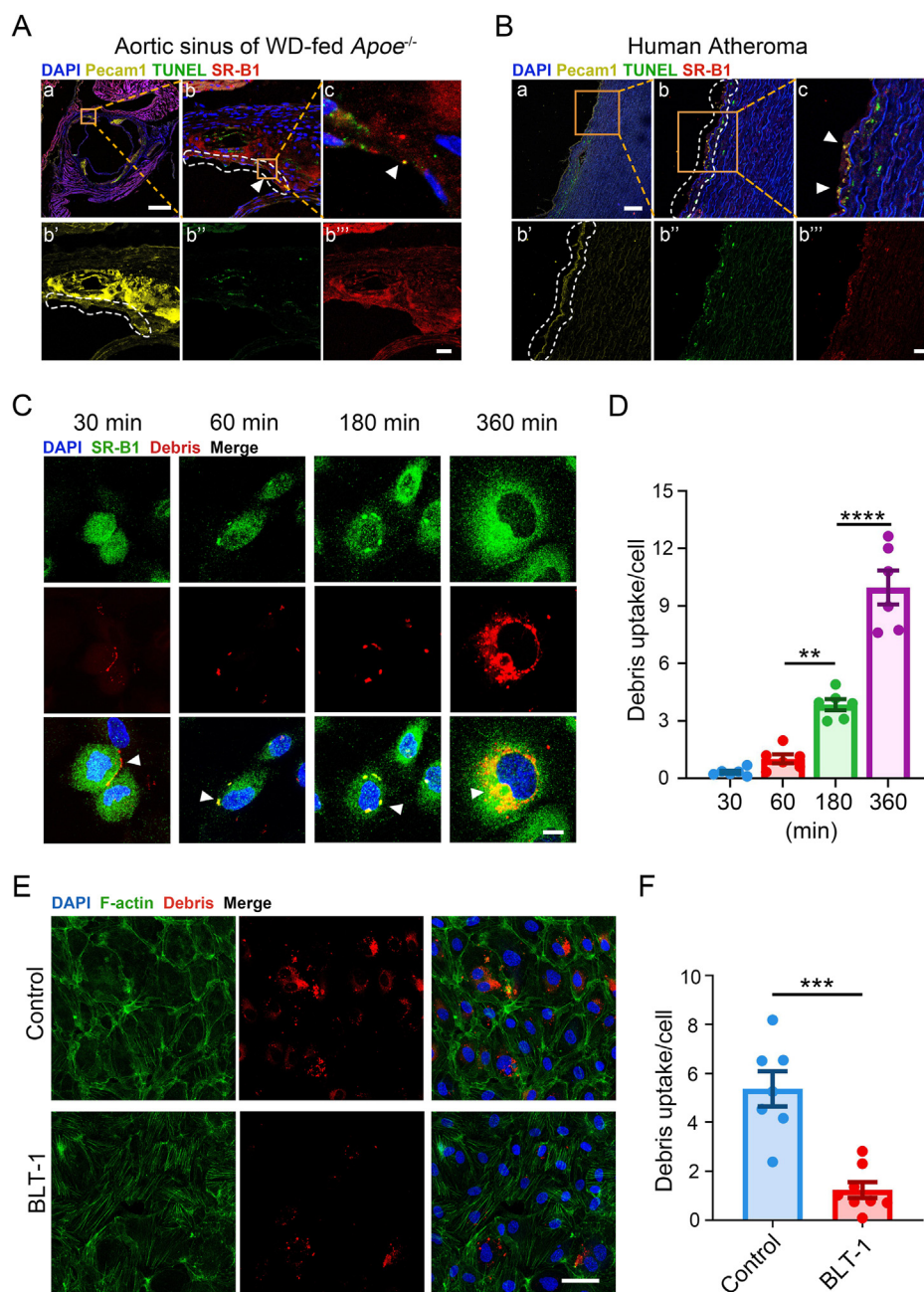

Figure 6 SR-B1 promoted apoptotic cell debris engulfment by vascular endothelial cells. **(A)** Internalization of apoptotic cell debris (TUNEL staining green) by SR-B1 (red) positive endothelial cells (Pecam1 staining yellow) in aortic roots of western diet (WD)-fed $Apoe^{-/-}$ mice. Top left scale bar, 500 μm; bottom right scale bar, 25 μm. **(B)** Internalization of apoptotic cell debris (TUNEL staining green) by SR-B1 (red) positive endothelial cells (Pecam1 staining yellow) in human atheroma of patients with atherosclerosis. Top left scale bar, 200 μm; bottom right scale bar, 25 μm. **(C)** The representative confocal images showing the engulfment of DiD-labeled cell debris (red) through SR-B1 (green) in primary human umbilical vein endothelial cells (pHUVECs) after exposure to cell debris for the indicated time points. Scale bar, 10 μm. **(D)** Quantification analysis of the number of cell debris in pHUVECs at the indicated time points ($n = 5$). **(E)** The representative confocal images showing the engulfment of DiD-labeled cell debris (red) by pHUVECs treated with or without 1 μM BLT-1 (SR-B1 inhibitor). Scale bar, 50 μm. **(F)** Quantification analysis of the number of cell debris in pHUVECs treated with or without BLT-1 ($n = 7$). The data were shown as mean ± standard error of the mean (error bars). **$P < 0.001$, ***$P < 0.001$, ****$P < 0.0001$.

showed that thick/reticular junctional morphology was the main VE-cadherin pattern (Fig. 5A—C). EC-engulfed debris led to an increase in both straight and finger junctions and loss of thick and reticular junctions, which indicated that VE-cadherin was transformed into an unstable condition and reorganized (Fig. 6A—C). Moreover, inhibiting SR-B1 could rescue VE-Cadherin instability during cell debris engulfment (Fig. 5A—C). Whereas, inhibiting SR-B1 could not rescue the expression level of VE-Cadherin during cell debris engulfment (Fig. 5D). Because the phagocytosis process is also related to the constant construction of actin cytoskeleton, we further analyzed the distribution of F-actin at the single cell level. We noticed that the distribution of cortical F-actin was significantly enhanced in pHUVECs co-cultured with cell debris and displayed a decrease in F-actin at cell periphery after inhibiting SR-B1 (Fig. 5E). Moreover, quantitative analysis of cell area and the distribution of F-actin showed that cell area was significantly increased after co-culture with cell debris in pHUVECs (Fig. 5F). Whereas, due to F-actin being accumulated in pericellular area, the distribution of F-actin was reduced during cell debris processing (Fig. 5G). Moreover, ECs co-cultured with cell debris displayed strongly defined F-actin immunofluorescence intensity (Fig. 5H; Fig. S8). As cytoskeleton and adherent junctions were important for ECs to migrate, we performed scratch-wound assays and found that the wound was completely closed at 24 h and less than approximately 30% of the wound area was healed after inhibiting SR-B1 (Fig. S9). These results indicated that SR-B1 was essential for cell adherent junction and cytoskeleton reorganization and might play an important role in engulfing cell debris.

Endothelial SR-B1 participates in the clearance of apoptotic cell debris in coronary artery

To determine the effect of endothelial SR-B1 on engulfing apoptotic cell debris, we detected the expression of SR-B1 on ECs. We first found that mouse endothelial SR-B1 was colocalized with TUNEL-labeled apoptotic cell debris in WD-fed $Apoe^{-/-}$ mice (Fig. 6A; Fig. S10A). Similarly, immunostaining of human atheroma tissues also showed that human SR-B1 was colocalized with TUNEL-labeled apoptotic cell debris in Pecam1$^+$ ECs (Fig. 6B; Fig. S10B). Furthermore, we explored the possible role of SR-B1 in engulfing cell debris. pHUVECs were utilized to co-culture with cell debris at different time points. Immunostaining showed that SR-B1 was colocalized with cell debris in pHUVECs after incubation with cell debris at different time points (Fig. 6C; Fig. S11). Respectively, the kinetics of cell debris engulfment by pHUVEC SR-B1 were started at 30 min and remained efficiently internalized until 360 min (Fig. 6C, D). These findings strongly suggested that SR-B1 was important for ECs to recognize apoptotic cell debris. We next used a selective SR-BI inhibitor BLT-1 to inhibit SR-B1-dependent selective phagocytosis[43] and found that endothelial SR-B1 participated in mediating the engulfment of cell debris. Qualificative analysis showed that the engulfment of cell debris by pHUVECs reduced by 75% under BLT-1 inhibition (Fig. 6E, F). Furthermore, after incubation with cell debris at different time points, the debris-laden pHUVECs were

quantified by flow cytometry and showed a dramatic decrease in their number under BLT-1 inhibition (Fig. S12). Moreover, we also found that inhibiting SR-B1 also reduced the transportation of lipid droplets and attenuated the transfer of debris to lysosomes. These data indicated that SR-B1 was important for ECs recognizing and engulfing apoptotic cell debris.

Discussion

Although professional phagocytes play a major role in clearing apoptotic cell debris, our results first demonstrated that vascular ECs act as non-professional phagocytic cells to engulf cell debris during atherosclerosis. Transcriptional profile analysis identified that endothelial SR-B1 was a key membrane receptor that mediated the engulfment of cell debris. Moreover, EC phagocytosis and processing of cell debris led to a series of events associated with cellular adherent junction and cytoskeleton reorganization.

The clearance of apoptotic cells and their debris is critical for maintaining vascular homeostasis. Atherosclerosis as a lipid-driven cardiovascular disease due to the accumulation of numerous foam cells and ensuing inflammation will result in the death of ECs, smooth muscle cells, and macrophages.[44] Most of our knowledge of apoptotic cell clearance was focused on professional phagocytes.[45] Whereas, with the unlimited accumulation of dead cells and expansion of the necrotic core in advanced atherosclerotic plaques, the dead cell clearance capacity of professional phagocytosis will be overwhelmed.[46] Meanwhile, macrophages will become defective phagocytosis due to excessive low-density lipoprotein accumulation and enhanced reactive oxygen species in advanced atherosclerotic plaque.[47] Recent studies have reported that smooth muscle cells can differentiate into macrophage-like cells in the advanced atherosclerotic plaques, which may play an important role in the process of debris clearance.[48,49] In previous work of our lab, we found that IgG-opsonized myelin debris can be engulfed by ECs during the early stages of spinal cord injury before macrophage recruitment.[13] Our study showed that ECs, a non-professional phagocytic cell type, had the ability to engulf apoptotic cell debris. Moreover, scRNA-seq analysis of atherosclerotic areas showed two distinct subpopulation ECs and enrichment of wounding-related pathways, which indicated that some ECs might be located in vulnerable/injured areas. Although it is well known that apoptotic cells can be cleared promptly in early atherosclerosis, the excessive accumulation of apoptotic cells leads to the forming of necrotic cores and makes atherosclerotic plaques vulnerable and injured.[5] We suspected that ECs might have a phagocytic subpopulation in vulnerable/injured areas during advanced atherosclerosis.

ECs, as a monolayer in vascular endothelium, play an important role in cellular adhesion, signal transduction, and barrier function which is the critical regulator for organ homeostasis.[50,51] Recent studies have demonstrated that transcytosis across the endothelium is essential for maintaining the influx and efflux of lipids, which is associated with lipoprotein transportation and the process of

atherosclerosis.[52,53] Here we found that endothelial SR-B1 was highly expressed in injured vascular cells and was enriched in phagocytosis-related pathway via RNA-seq analysis. Moreover, the scRNA-seq analysis also demonstrated that SR-B1 was highly expressed in a single EC subpopulation, which showed that SR-B1-positive ECs might have unique biological functions and characters. GO enrichment analysis showed that adherent junction- and cytoskeleton-related genes had dramatically changed in the SR-B1-positive EC subpopulation. Researchers have reported that the reorganization of cortical cytoskeleton and adherent junctions is critical for anchoring transmembrane proteins to control their movements and priming the engagement between receptors and target particles via extensive ruffling.[37,54,55] Furthermore, the polymerization of actin also plays an important role in increasing cortical tension to promote membrane fusion during phagocytosis.[39,56] Here, our studies showed that cell debris can activate the reorganization of cytoskeleton and adherent junctions in SR-B1-positive ECs. Meanwhile, inhibiting SR-B1 showed a low rate of adherent junction and cytoskeleton reorganization during co-culture with cell debris. SR-B1 is considered the LDL binding receptor, which mediates the bidirectional flux of cholesterol.[18] Moreover, researchers have found that SR-B1 can recognize plasma membrane cholesterol and stimulate intracellular signaling to internalize cholesterol.[57] Using fluorescent labeling of cell debris, we showed that SR-B1 as a selective receptor was involved in cell debris engulfment by ECs. These results indicated that SR-B1 had the novel capacity to interact with cell debris and played a receptor function in debris internalization.

In conclusion, we revealed that ECs acted as non-professional phagocytes to engulf apoptotic cell debris during atherosclerosis. In order to further detect the mechanism of the process of endothelial phagocytosis, scRNA-seq and bulk RNA-seq datasets were utilized to analyze the changes in the biological process during atherosclerosis. We found that SR-B1 as an endothelium-specific expressed gene was enriched in the phagocytosis-related pathway. Moreover, we further assessed the unique character of SR-B1 highly expressed cells in arteries at the single cell level and found that SR-B1-positive ECs were a separating subpopulation, which had different biological functions on cellular adherent junction and cytoskeleton reorganization. Given our finding that SR-B1 was essential for the engulfment of apoptotic cell debris, these data suggested that endothelial SR-B1 associated with the reorganization of cellular adherent junctions and cytoskeleton was the key receptor of apoptotic cell debris clearance in the coronary artery.

Author contributions

G. Wang, J. Qiu, and J. Xu conceived the idea and designed the experiments. J. Xu and J. Wang performed experiments, and analyzed, computed, and interpreted the data. H. Zhang, Y. Chen, and X. Zhang assisted experiments. M. Xie, Y. Zhang, and J. Xiao collected and processed the histological data. G. Wang, J. Qiu, and J. Xu wrote and revised the article. G. Wang made final approval of the article.

Conflict of interests

The authors declared that there was no financial conflict of interests.

Funding

Data availability

All data that are not contained in this manuscript and supplementary materials are available from the corresponding authors upon reasonable request.

Acknowledgements

Appendix A. Supplementary data

Supplementary data to this article can be found online at https://doi.org/10.1016/j.gendis.2024.101250.

References

1. Tabas I, Williams KJ, Borén J. Subendothelial lipoprotein retention as the initiating process in atherosclerosis: update and therapeutic implications. *Circulation*. 2007;116(16): 1832−1844.
2. Chistiakov DA, Melnichenko AA, Myasoedova VA, Grechko AV, Orekhov AN. Mechanisms of foam cell formation in atherosclerosis. *J Mol Med*. 2017;95(11):1153−1165.
3. Doddapattar P, Dev R, Ghatge M, et al. Myeloid cell PKM2 deletion enhances efferocytosis and reduces atherosclerosis. *Circ Res*. 2022;130(9):1289−1305.
4. Hassan A, Din AU, Zhu Y, et al. Anti-atherosclerotic effects of *Lactobacillus plantarum* ATCC 14917 in ApoE⁻/⁻ mice through modulation of proinflammatory cytokines and oxidative stress. *Appl Microbiol Biotechnol*. 2020;104(14): 6337−6350.
5. Finn AV, Nakano M, Narula J, Kolodgie FD, Virmani R. Concept of vulnerable/unstable plaque. *Arterioscler Thromb Vasc Biol*. 2010;30(7):1282−1292.
6. Naghavi M, Libby P, Falk E, et al. From vulnerable plaque to vulnerable patient: a call for new definitions and risk assessment strategies: Part II. *Circulation*. 2003;108(15): 1772−1778.
7. Arandjelovic S, Ravichandran KS. Phagocytosis of apoptotic cells in homeostasis. *Nat Immunol*. 2015;16(9):907−917.

8. Hünniger K, Kurzai O. Phagocytes as central players in the defence against invasive fungal infection. *Semin Cell Dev Biol*. 2019;89:3—15.

9. Dale DC, Boxer L, Liles WC. The phagocytes: neutrophils and monocytes. *Blood*. 2008;112(4):935—945.

10. Han CZ, Juncadella IJ, Kinchen JM, et al. Macrophages redirect phagocytosis by non-professional phagocytes and influence inflammation. *Nature*. 2016;539(7630):570—574.

11. Cabrera JTO, Makino A. Efferocytosis of vascular cells in cardiovascular disease. *Pharmacol Ther*. 2022;229:107919.

12. Hoijman E, Häkkinen HM, Tolosa-Ramon Q, et al. Cooperative epithelial phagocytosis enables error correction in the early embryo. *Nature*. 2021;590(7847):618—623.

13. Zhou T, Zheng Y, Sun L, et al. Microvascular endothelial cells engulf myelin debris and promote macrophage recruitment and fibrosis after neural injury. *Nat Neurosci*. 2019;22(3): 421—435.

14. Schrijvers DM, De Meyer GRY, Kockx MM, Herman AG, Martinet W. Phagocytosis of apoptotic cells by macrophages is impaired in atherosclerosis. *Arterioscler Thromb Vasc Biol*. 2005;25(6):1256—1261.

15. Kiefer C, Sumser E, Wernet MF, Von Lintig J. A class B scavenger receptor mediates the cellular uptake of carotenoids in *Drosophila*. *Proc Natl Acad Sci U S A*. 2002;99(16): 10581—10586.

16. Sakudoh T, Iizuka T, Narukawa J, et al. A CD36-related transmembrane protein is coordinated with an intracellular lipid-binding protein in selective carotenoid transport for cocoon coloration. *J Biol Chem*. 2010;285(10):7739—7751.

17. Braun A, Trigatti BL, Post MJ, et al. Loss of SR-BI expression leads to the early onset of occlusive atherosclerotic coronary artery disease, spontaneous myocardial infarctions, severe cardiac dysfunction, and premature death in apolipoprotein E-deficient mice. *Circ Res*. 2002;90(3):270—276.

18. Huang L, Chambliss KL, Gao X, et al. SR-B1 drives endothelial cell LDL transcytosis via DOCK4 to promote atherosclerosis. *Nature*. 2019;569(7757):565—569.

19. Tao H, Yancey PG, Babaev VR, et al. Macrophage SR-BI mediates efferocytosis via Src/PI3K/Rac1 signaling and reduces atherosclerotic lesion necrosis. *J Lipid Res*. 2015;56(8): 1449—1460.

20. Pan H, Xue C, Auerbach BJ, et al. Single-cell genomics reveals a novel cell state during smooth muscle cell phenotypic switching and potential therapeutic targets for atherosclerosis in mouse and human. *Circulation*. 2020;142(21): 2060—2075.

21. Kalluri AS, Vellarikkal SK, Edelman ER, et al. Single-cell analysis of the normal mouse aorta reveals functionally distinct endothelial cell populations. *Circulation*. 2019;140(2): 147—163.

22. Hao Y, Hao S, Andersen-Nissen E, et al. Integrated analysis of multimodal single-cell data. *Cell*. 2021;184(13): 3573—3587.e29.

23. McDonald AI, Shirali AS, Aragón R, et al. Endothelial regeneration of large vessels is a biphasic process driven by local cells with distinct proliferative capacities. *Cell Stem Cell*. 2018; 23(2):210—225.e6.

24. Bao H, Li ZT, Xu LH, et al. Platelet-derived extracellular vesicles increase Col8a1 secretion and vascular stiffness in intimal injury. *Front Cell Dev Biol*. 2021;9:641763.

25. Dunn J, Qiu H, Kim S, et al. Flow-dependent epigenetic DNA methylation regulates endothelial gene expression and atherosclerosis. *J Clin Invest*. 2014;124(7):3187—3199.

26. Ritchie ME, Phipson B, Wu D, et al. Limma powers differential expression analyses for RNA-sequencing and microarray studies. *Nucleic Acids Res*. 2015;43(7):e47.

27. Robinson MD, McCarthy DJ, Smyth GK, edgeR. A bioconductor package for differential expression analysis of digital gene expression data. *Bioinformatics*. 2010;26(1):139—140.

28. Yu G, Wang LG, Han Y, He QY. clusterProfiler: an R package for comparing biological themes among gene clusters. *OMICS*. 2012;16(5):284—287.

29. Henson PM, Bratton DL, Fadok VA. Apoptotic cell removal. *Curr Biol*. 2001;11(19):R795—R805.

30. Moore KJ, Tabas I. Macrophages in the pathogenesis of atherosclerosis. *Cell*. 2011;145(3):341—355.

31. Gene Ontology Consortium. Gene ontology consortium: going forward. *Nucleic Acids Res*. 2015;43(Database issue): D1049—D1056.

32. Huang DW, Sherman BT, Lempicki RA. Systematic and integrative analysis of large gene lists using DAVID bioinformatics resources. *Nat Protoc*. 2009;4(1):44—57.

33. Pierce JB, Feinberg MW. Long noncoding RNAs in atherosclerosis and vascular injury: pathobiology, biomarkers, and targets for therapy. *Arterioscler Thromb Vasc Biol*. 2020;40(9):2002—2017.

34. Fu Y, Wang X, Kong W. Hyperhomocysteinaemia and vascular injury: advances in mechanisms and drug targets. *Br J Pharmacol*. 2018;175(8):1173—1189.

35. Förstermann U, Xia N, Li H. Roles of vascular oxidative stress and nitric oxide in the pathogenesis of atherosclerosis. *Circ Res*. 2017;120(4):713—735.

36. Hsu PL, Chen JS, Wang CY, Wu HL, Mo FE. Shear-induced CCN_1 promotes atheroprone endothelial phenotypes and atherosclerosis. *Circulation*. 2019;139(25):2877—2891.

37. Fornetti J, Flanders KC, Henson PM, Tan AC, Borges VF, Schedin P. Mammary epithelial cell phagocytosis downstream of TGF-β3 is characterized by adherens junction reorganization. *Cell Death Differ*. 2016;23(2):185—196.

38. Stahnke S, Döring H, Kusch C, et al. Loss of Hem1 disrupts macrophage function and impacts migration, phagocytosis, and integrin-mediated adhesion. *Curr Biol*. 2021;31(10): 2051—2064.e8.

39. Mylvaganam S, Freeman SA, Grinstein S. The cytoskeleton in phagocytosis and macropinocytosis. *Curr Biol*. 2021;31(10): R619—R632.

40. Giannotta M, Trani M, Dejana E. VE-cadherin and endothelial adherens junctions: active guardians of vascular integrity. *Dev Cell*. 2013;26(5):441—454.

41. Neto F, Klaus-Bergmann A, Ong YT, et al. YAP and TAZ regulate adherens junction dynamics and endothelial cell distribution during vascular development. *Elife*. 2018;7:e31037.

42. Qu K, Wang C, Huang L, et al. TET1s deficiency exacerbates oscillatory shear flow-induced atherosclerosis. *Int J Biol Sci*. 2022;18(5):2163—2180.

43. Nieland TJF, Penman M, Dori L, Krieger M, Kirchhausen T. Discovery of chemical inhibitors of the selective transfer of lipids mediated by the HDL receptor SR-BI. *Proc Natl Acad Sci U S A*. 2002;99(24):15422—15427.

44. Rayner KJ. Cell death in the vessel wall: the good, the bad, the ugly. *Arterioscler Thromb Vasc Biol*. 2017;37(7):e75—e81.

45. Kourtzelis I, Hajishengallis G, Chavakis T. Phagocytosis of apoptotic cells in resolution of inflammation. *Front Immunol*. 2020;11:553.

46. Dhawan UK, Singhal A, Subramanian M. Dead cell and debris clearance in the atherosclerotic plaque: mechanisms and therapeutic opportunities to promote inflammation resolution. *Pharmacol Res*. 2021;170:105699.

47. Yan J, Horng T. Lipid metabolism in regulation of macrophage functions. *Trends Cell Biol*. 2020;30(12):979—989.

48. Misra A, Feng Z, Chandran RR, et al. Integrin beta3 regulates clonality and fate of smooth muscle-derived atherosclerotic plaque cells. *Nat Commun*. 2018;9(1):2073.

49. Li Y, Zhu H, Zhang Q, et al. Smooth muscle-derived macrophage-like cells contribute to multiple cell lineages in the atherosclerotic plaque. *Cell Discov.* 2021;7(1):111.

50. Marziano C, Genet G, Hirschi KK. Vascular endothelial cell specification in health and disease. *Angiogenesis.* 2021;24(2):213—236.

51. Reglero-Real N, Colom B, Bodkin JV, Nourshargh S. Endothelial cell junctional adhesion molecules: role and regulation of expression in inflammation. *Arterioscler Thromb Vasc Biol.* 2016;36(10):2048—2057.

52. Ramírez CM, Zhang X, Bandyopadhyay C, et al. Caveolin-1 regulates atherogenesis by attenuating low-density lipoprotein transcytosis and vascular inflammation independently of endothelial nitric oxide synthase activation. *Circulation.* 2019; 140(3):225—239.

53. Bai X, Yang X, Jia X, et al. CAV1-CAVIN1-LC3B-mediated autophagy regulates high glucose-stimulated LDL transcytosis. *Autophagy.* 2020;16(6):1111—1129.

54. Mylvaganam SM, Grinstein S, Freeman SA. Picket-fences in the plasma membrane: functions in immune cells and phagocytosis. *Semin Immunopathol.* 2018;40(6):605—615.

55. Freeman SA, Vega A, Riedl M, et al. Transmembrane pickets connect cyto- and pericellular skeletons forming barriers to receptor engagement. *Cell.* 2018;172(1—2): 305—317.e10.

56. Hall AB, Gakidis MM, Glogauer M, et al. Requirements for Vav guanine nucleotide exchange factors and Rho GTPases in FcgammaR- and complement-mediated phagocytosis. *Immunity.* 2006;24(3):305—316.

57. Saddar S, Carriere V, Lee WR, et al. Scavenger receptor class B type I is a plasma membrane cholesterol sensor. *Circ Res.* 2013; 112(1):140—151.